

# Physical and geometrical parameters of CVBS X: the spectroscopic binary Gliese 762.1

Suhail G. Masda<sup>1</sup>, Mashhoor A. Al-Wardat<sup>2</sup>, Ralph Neuhäuser<sup>1</sup> and Hamid M. Al-Naimiy<sup>3</sup>

<sup>1</sup> Astrophysikalisches Institut und Universitäts-Sternwarte Jena, FSU Jena, 07745 Jena, Germany

<sup>2</sup> Physics Department, Faculty of Science, Al al-Bayt University, PO Box: 130040, Mafrqa, 25113 Jordan;  
mwardat@aabu.edu.jo

<sup>3</sup> Applied Physics and Space Science Department, University of Sharjah PO Box: 27272 Sharjah, United Arab Emirates

Received 2015 December 3; accepted 2016 March 10

**Abstract** We present the physical and geometrical parameters of the individual components of the close visual double-lined spectroscopic binary system Gliese 762.1, which were estimated using Al-Wardat's complex method for analyzing close visual binary systems. The estimated parameters of the individual components of the system are as follows: radius  $R_A = 0.845 \pm 0.09 R_\odot$ ,  $R_B = 0.795 \pm 0.10 R_\odot$ , effective temperature  $T_{\text{eff}}^A = 5300 \pm 50$  K,  $T_{\text{eff}}^B = 5150 \pm 50$  K, surface gravity  $\log g_A = 4.52 \pm 0.10$ ,  $\log g_B = 4.54 \pm 0.15$  and luminosity  $L_A = 0.51 \pm 0.08 L_\odot$ ,  $L_B = 0.40 \pm 0.07 L_\odot$ . New orbital elements are presented with a semi-major axis of  $0.0865 \pm 0.010$  arcsec using the Hipparcos parallax  $\pi = 58.96 \pm 0.65$  mas, and an accurate total mass and individual masses of the system are determined as  $M = 1.72 \pm 0.60 M_\odot$ ,  $M_A = 0.89 \pm 0.08 M_\odot$  and  $M_B = 0.83 \pm 0.07 M_\odot$ . Finally, the spectral types and luminosity classes of both components are assigned as K0V and K1.5V for the primary and secondary components respectively, and their positions on the H-R diagram and evolutionary tracks are given.

**Key words:** stars: fundamental parameters — binaries: spectroscopic binary system — atmospheres modeling — Gliese 762.1

## 1 INTRODUCTION

The importance of the study of binary stars arises from the fact that more than 50% of nearby solar-type main sequence stars are binary or multiple stellar systems (the fraction is 42% among nearby M stars, Duquenooy et al. 1991) and several astronomical phenomena occur only in binary stars. They provide a source of direct measurements of stellar parameters or Galactic quantities. Stellar physics needs masses, luminosities and radii obtained through the studies of binary stars. Galactic physics also benefits from these studies, e.g. the Galactic potential can be tested using wide binaries, and chemical evolution depends on binaries through the process of Type Ia supernovae (Arenou et al. 2002). The mass-luminosity relation of low-mass main sequence stars in the solar neighborhood are known with much lower accuracy than those of massive early-type stars (Balega et al. 2002, 2007b; Forveille et al. 1999). This requires precise determination of their masses and luminosities.

Close visual binary stars (CVBSs) are so close that they cannot be visually resolved except through special techniques like speckle interferometry or by deducing their duplicity using high resolution spectroscopy. So, these cases are somewhat more complicated and need indirect

methods to estimate their physical and geometrical parameters.

Combining observational measurements with stellar theoretical models is the most powerful indirect method to analyze such binary and multiple systems. This was implemented in Al-Wardat's complex method (Al-Wardat 2007), which combines magnitude difference measurements of speckle interferometry, the entire spectral energy distribution (SED) derived through spectrophotometry, and radial velocity measurements, along with modeling the atmospheres to estimate the individual physical parameters. In coordination with these physical parameters, the geometrical parameters and their errors are calculated using a modern version of Tokovinin's ORBITX program, which depends on the standard least-squares method (Tokovinin 1992).

The method was firstly introduced by Al-Wardat (2002a, 2007) (henceforth paper I and paper II in this series respectively), where it was applied to the analysis of the quadruple hierarchical system ADS 11061 and the two binary systems COU 1289 and COU 1291. Later on, the method was successfully applied to several solar-type and subgiant binary systems: Hip 11352, Hip 11253 and Hip 689 (Al-Wardat & Widyana 2009; Al-Wardat 2009, 2012) (henceforth papers III, IV and V in this series respectively).

The method was then developed to be more sophisticated and powerful by combining the physical solution with the geometrical one represented by the orbital solution of the system. This approach was applied to the systems: HD 25811, HD 375, Gliese 150.5 and HD 6009 (Al-Wardat et al. 2014a,b,c; Al-Wardat 2014) (henceforth papers VI, VII, VIII and IX in this series respectively).

In order to be analyzed using Al-Wardat’s method, a binary system should have a magnitude difference measurement, an entire observed SED covering the optical range, and an entire precise optical (UBV) photometric magnitude measurement. The procedure starts with calculating the individual flux of each component using the magnitude difference with the entire photometrical magnitude, then estimating their preliminary effective temperatures and gravity accelerations in order to build their SED using grids of Kurucz (1994) blanketed models (ATLAS9). These two models in turn are used to build an entire synthetic SED for the system, which is compared with the observational one in an iterative way until the best fit is achieved. Of course there should be agreement between the masses calculated using the physical solution and those calculated using the orbital one, otherwise a new set of parameters should be tested.

This is the tenth paper in this series. Here, we provide a complete analysis of the CVBS Gliese 762.1 using Al-Wardat’s complex method.

Gliese 762.1 (MCA 56 AB = WDS J19311+5835 = GJ 762.1 = HD 184467 = HIP 95995) was first visually resolved by McAlister et al. (1983). It is a well known double-lined spectroscopic binary (SB2 Pourbaix & Jorissen 2000), with an orbital period of 1.35 year (Batten et al. 1989). It shines at an apparent visual magnitude of  $m_v = 6.60^m$  and the spectral types of both components are cataloged as K2V and K4V for the primary and secondary components respectively (Farrington et al. 2010). Hipparcos trigonometric parallax measurement of the system,  $\pi = 58.96 \pm 0.65$  mas (van Leeuwen 2007), places this system at a distance of 16.96 pc, making it a nearby K-type star.

Table 1 contains basic data of the system Gliese 762.1 from the SIMBAD, NASA/IPAC, Hipparcos and Tycho Catalogs (ESA 1997).

## 2 ANALYSIS OF THE SYSTEM

### 2.1 Modeling the Atmospheres and Estimation of the Physical Parameters

In spite of the fact that duplicity of the system was detected using high resolution spectroscopy and speckle interferometry, the system is seen as a single star even with the aid of the biggest telescopes. So, in order to estimate the physical parameters of the individual components of the system, we apply Al-Wardat’s complex method for analyzing a CVBS. The synthetic SEDs of individual components of the system are computed using ATLAS9 line blanketed model atmospheres from Kurucz (1994) using a special subroutine.

**Table 1** Basic data of the system Gliese 762.1 from SIMBAD, NASA/IPAC, Hipparcos and Tycho Catalogs.

Parameter	GJ 762.1	Source of Data
$\alpha_{2000}$ †	19 <sup>h</sup> 31 <sup>m</sup> 07.974 <sup>s</sup>	SIMBAD
$\delta_{2000}$ ‡	+58°35′09.64″	-
HIP	95995	-
Sp. Typ.	K1V	-
$E(B - V)^*$	$0.07 \pm 0.002$	NASA/IPAC
$A_v^*$	$0.21^m$	NASA/IPAC
$B_J$ (Hip)	$7.46^m$	Hipparcos
$V_J$ (Hip)	$6.60^m$	-
$R_J$ (Hip)	$6.10^m$	-
$(B - V)_J$ (Hip)	$0.86^m \pm 0.001$	-
$(U - B)_J$	$0.52^m \pm 0.001$	-
$B_T$	$7.71^m \pm 0.006$	Tycho
$V_T$	$6.71^m \pm 0.005$	-
$(B - V)_J$ (Tyc)	$0.87^m \pm 0.006$	-
$\pi_{Hip}$ (mas)	$59.84 \pm 0.64$	Hipparcos
$\pi_{Tyc}$ (mas)	$58.00 \pm 2.90$	Tycho
$\pi_{Hip}^*$ (mas)	$58.96 \pm 0.65$	New Hipparcos

Notes: † Right Ascension; ‡ Declination; \* <http://irsa.ipac.caltech.edu/>; \*\* van Leeuwen (2007)

In order to build the model atmospheres of each of the components, we need preliminary input parameters ( $T_{\text{eff}}$  and  $\log g$ ). These are calculated as follows:

Using the apparent visual magnitude of the system  $m_v = 6.60^m$  from previous data (Table 1), and the visual magnitude difference  $\Delta m = 0.33^m \pm 0.06$  between the two components as the average of fifteen  $\Delta m$  measurements of the filters  $\lambda$  503 – 850 (Table 2), we calculated a preliminary individual  $m_v$  for each component using the following equations

$$\begin{aligned} m_A &= m_v + 2.5 \log(1 + 10^{-0.4\Delta m}), \\ m_B &= m_A + \Delta m, \end{aligned} \quad (1)$$

which give

$$m_v^A = 7.20^m \pm 0.03, \quad m_v^B = 7.53^m \pm 0.07.$$

Combining these magnitudes with the Hipparcos trigonometric parallax ( $\pi_{Hip}$ ) from van Leeuwen (2007), we can derive the preliminary absolute magnitudes for the components using the following relation

$$M_V = m_v + 5 - 5 \log(d) - A_v. \quad (2)$$

$M_V^A = 5.85^m \pm 0.04$  and  $M_V^B = 6.18^m \pm 0.07$ , where  $A_v$  is the interstellar reddening which was taken from NASA/IPAC (See Table 1).

The bolometric corrections, bolometric magnitudes and stellar luminosities of the system were taken from Lang (1992) and Gray (2005). These values, along with the following two equations

$$\begin{aligned} \log(R/R_\odot) &= 0.5 \log(L/L_\odot) - 2 \log(T_{\text{eff}}/T_\odot), \quad (3) \\ \log g &= \log(M/M_\odot) \\ &\quad - 2 \log(R/R_\odot) + 4.43 \end{aligned} \quad (4)$$

were used to calculate the preliminary input parameters as  $T_{\text{eff}}^A = 5300$  K,  $T_{\text{eff}}^B = 5050$  K,  $\log g_A = 4.56$ ,  $\log g_B =$

**Table 2** Magnitude difference between the components of the system Gliese 762.1, along with filters used to obtain the observations.

$\Delta m$ (mag)	$\sigma_{\Delta m}$	Filter ( $\lambda/\Delta\lambda$ )	Reference
0.26	0.05	545 nm/30	[1]
0.33	0.07	545 nm/30	[2]
0.27	0.04	610 nm/20	[3]
0.27	0.15	648 nm/41	[4]
0.32	0.15	503 nm/40	[4]
0.24	0.02	545 nm/30	[5]
0.25	0.19	600 nm/30	[5]
0.24	0.31	850 nm/75	[5]
0.41	–	698 nm/39	[6]
0.29	0.03	600 nm/30	[7]
0.73	–	698 nm/39	[6]
0.53	–	550 nm/40	[6]
0.27	–	754 nm/44	[6]
0.19	–	562 nm/40	[8]
0.28	–	692 nm/40	[8]

Notes: [1] Pluzhnik (2005); [2] Balega et al. (2002); [3] Balega et al. (2004); [4] Horch et al. (2004); [5] Balega et al. (2006); [6] Horch et al. (2008); [7] Balega et al. (2007a); [8] Horch et al. (2011).

4.54,  $R_A = 0.815R_\odot$  and  $R_B = 0.806R_\odot$ .  $T_\odot$  was taken as 5777 K.

The entire synthetic SED as if it were received from the system and measured above the Earth’s atmosphere is calculated using the following equations

$$F_\lambda \cdot d^2 = H_\lambda^A \cdot R_A^2 + H_\lambda^B \cdot R_B^2, \quad (5)$$

from which

$$F_\lambda = (R_A/d)^2 (H_\lambda^A + H_\lambda^B \cdot (R_B/R_A)^2), \quad (6)$$

where  $R_A$  and  $R_B$  are the radii of the primary and secondary components of the system in solar units respectively,  $H_\lambda^A$  and  $H_\lambda^B$  are the fluxes at the surfaces of the stars and  $F_\lambda$  is the flux for the entire SED of the system above the Earth’s atmosphere, which is located at a distance  $d$  (pc) from the system.

The exact physical parameters of the components of the system are those which lead to the best fit between the entire synthetic SED and the observational one. This was taken from Al-Wardat (2002b). The observational spectrum (Fig. 1) was obtained using a low resolution grating (325/4° grooves/mm, Å/pixel reciprocal dispersion) within the UAGS spectrograph at the 1 m (Zeiss-1000) SAO-Russian telescope.

In addition to the visual best fit between the two spectra, the synthetic magnitudes, color indices and line profiles, especially those of hydrogen  $H_\beta$ (4861.33Å),  $H_\gamma$ (4340.5Å) and  $H_\delta$ (4101Å), should fit the observed ones. Otherwise, a new set of parameters should be tested in an iterative way until the best fit is reached.

The best fit (Fig. 1) was achieved using the parameters shown in Table 4. The luminosities and masses of the components were calculated using Equations (3) and (4), and the spectral types of the components in the system were

**Table 3** Relative position measurements obtained with different methods, which are used to construct the orbit of the system. These points are taken from the Fourth Catalog of Interferometric Measurements of Binary Stars.

Epoch	$\theta$ (°)	$\rho$ (arcsec)	Reference
1980.4797	254.2	0.117	McA1983 [1]
1980.7228	226.7	0.106	McA1983 [1]
1981.4736	310.4	0.081	McA1984a [2]
1983.4175	225.8	0.115	McA1987b [3]
1984.7039	235.7	0.112	McA1987b [3]
1985.4900	322.4	0.066	McA1987b [3]
1985.7390	273.1	0.104	Tok1988 [5]
1986.8883	308.5	0.065	McA1989 [6]
1987.7618	172.7	0.067	McA1989 [6]
1989.7059	286.0	0.093	Hrt1992b [7]
1989.8041	272.2	0.100	Bag1994 [8]
1989.8096	268.2	0.102	Bag1994 [8]
1990.4322	171.6	0.062	Ism1992 [9]
1991.25	284.0	0.100	HIP1997a [10]
1993.8438	271.3	0.102	Bag1994 [8]
1994.7080	292.1	0.062	Hrt2000a [11]
1995.4397	244.8	0.113	Hrt1997 [12]
1995.7621	201.9	0.086	Hrt1997 [12]
1996.6903	255.0	0.111	Hrt1997 [12]
1999.8179	204.1	0.086	Bag2002 [13]
2000.6166	271.9	0.099	Bag2004 [14]
2000.7640	253.8	0.111	Hor2002a [15]
2001.7550	134.6	0.065	Bag2006b [16]
2003.6339	235.6	0.114	Hor2008 [17]
2004.8150	75.0	0.110	Bag2007b [18]
2005.7662	153.5	0.054	CIA2010 [19]
2006.4381	44.9	0.104	Bag2013 [20]
2006.5198	211.3	0.098	Hor2008 [17]
2006.5227	213.8	0.095	Hor2008 [17]
2007.8011	46.0	0.112	Hrt2009 [21]
2010.4816	227.6	0.106	Hor2011 [22]

Notes: [1] McAlister et al. (1983), [2] McAlister et al. (1984), [3] McAlister et al. (1987), [4] Tokovinin (1985), [5] Tokovinin & Ismailov (1988), [6] McAlister et al. (1989), [7] Hartkopf et al. (1992), [8] Balega et al. (1994), [9] Ismailov (1992), [10] ESA (1997), [11] Hartkopf et al. (2000), [12] Hartkopf et al. (1997), [13] Balega et al. (2002), [14] Balega et al. (2004), [15] Horch et al. (2002), [16] Balega et al. (2006), [17] Horch et al. (2008), [18] Balega et al. (2007a), [19] Farrington et al. (2010), [20] Balega et al. (2013), [21] Hartkopf & Mason (2009), [22] Horch et al. (2011).

derived from the empirical  $Sp - M_V$  relation for main sequence stars provided by Lang (1992).

## 2.2 Orbital Solution and Masses

Once available, the orbital elements of a binary system would enhance and help in examining the physical parameters of its individual components. The sum of the masses of the two components given by Equations (7) and (8) should coincide with that estimated from their positions on the evolutionary tracks and that calculated using the empirical equations and standard tables.

We followed Tokovinin’s method (Tokovinin 1992) to calculate the orbital elements. The method performs a least-squares adjustment to all available radial velocity and

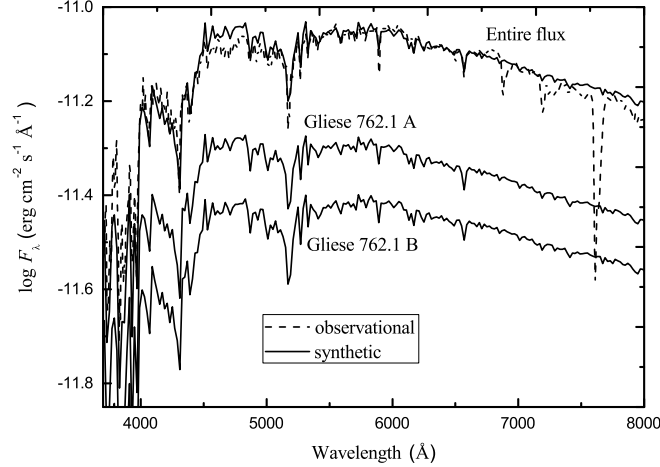


**Fig. 1** Best fit between the entire observed SED (*dashed line*), which was taken from (Al-Wardat 2002b), and the entire synthetic SED (solid line) for the system Gliese 762.1. Individual synthetic SEDs were computed using  $T_{\text{eff}}^A = 5300 \pm 50$  K,  $\log g_A = 4.56 \pm 0.10$ ,  $R_A = 0.815 \pm 0.09 R_{\odot}$ ,  $T_{\text{eff}}^B = 5150 \pm 50$  K,  $\log g_B = 4.54 \pm 0.10$  and  $R_B = 0.806 \pm 0.10 R_{\odot}$ , with  $d = 16.96$  pc ( $\pi = 58.96 \pm 0.65$  mas).

**Table 4** Fundamental parameters of the components of the system Gliese 762.1.

Parameters	Comp. A	Comp. B
$T_{\text{eff}}$ (K)	$5300 \pm 50$	$5150 \pm 50$
Radius ( $R_{\odot}$ )	$0.845 \pm 0.09$	$0.795 \pm 0.10$
$\log g$	$4.52 \pm 0.10$	$4.54 \pm 0.15$
$L(L_{\odot})$	$0.51 \pm 0.08$	$0.40 \pm 0.07$
$M_{\text{bol}}$	$5.48^{\text{m}} \pm 0.90$	$5.74^{\text{m}} \pm 1.02$
$M_V$	$5.85^{\text{m}} \pm 0.80$	$6.18^{\text{m}} \pm 0.85$
Mass ( $M_{\odot}$ )*	$0.89 \pm 0.08$	$0.83 \pm 0.07$
Sp. Type**	K0	K1.5
Parallax (mas)	$58.96 \pm 0.65$	
$(\frac{M_A + M_B}{M_{\odot}})^{***}$	$1.72 \pm 0.60$	
Age (Gyr)	$9 \pm 1$	

Notes: \*depending on Eq. (4), \*\*depending on the tables in Lang (1992), \*\*\*depending on the orbital solution.

relative position observations, with weights inversely proportional to the square of their standard errors. The orbital solution involves: the orbital period,  $P$ ; the semi-amplitudes of the primary and secondary velocities,  $K1$  and  $K2$  respectively; the eccentricity,  $e$ ; the semi-major axis,  $a$ ; the center of mass velocity,  $\gamma$ ; and the time of primary minimum,  $T_0$ . The radial velocities for the system were taken from McClure (1983).

Table 5 lists the results of the radial-velocity solution (Fig. 2). The best orbit that passes through the relative position measurements is shown in Figure 3 and the resulting orbital elements are compared with earlier studies in Table 6.

The estimated orbital elements, semi-major axis, orbital period (see Table 6), and Hipparcos parallax from van Leeuwen (2007) ( $\pi = 58.96 \pm 0.65$  mas), along with

**Table 5** Orbital solution of the system using the velocity curves shown in Fig. 2.

Parameters	McClure (1983)	This paper
$P$ (yr)	$1.3477 \pm 0.0038$	$1.3534 \pm 0.0010$
$T_0$ (MJD)	$44194.3 \pm 3.2$	$47670.20 \pm 2.01$
$e$	$0.416 \pm 0.016$	$0.40 \pm 0.013$
$\omega$ ( $^{\circ}$ )	$177.1 \pm 2.70$	$179.0 \pm 2.24$
$K1$ ( $\text{km s}^{-1}$ )	$9.52 \pm 0.16$	$9.40 \pm 0.12$
$K2$ ( $\text{km s}^{-1}$ )	$10.46 \pm 0.19$	$10.35 \pm 0.19$
$V_{\gamma}$ ( $\text{km s}^{-1}$ )	$11.41 \pm 0.014$	$11.31 \pm 0.12$

Kepler's third law:

$$M_A + M_B = \left( \frac{a^3}{\pi^3 P^2} \right) M_{\odot}, \quad (7)$$

$$\frac{\sigma_M}{M} = \sqrt{\left( 3 \frac{\sigma_{\pi}}{\pi} \right)^2 + \left( 3 \frac{\sigma_a}{a} \right)^2 + \left( 2 \frac{\sigma_P}{P} \right)^2}, \quad (8)$$

yield a mass sum with its corresponding error for the system of  $M_A + M_B = 1.72 \pm 0.60 M_{\odot}$ . Using atmospheric modeling Equation (4), the total mass of the system is  $1.69 \pm 0.22 M_{\odot}$ .

### 3 SYNTHETIC PHOTOMETRY

The entire and individual synthetic magnitudes are calculated by integrating the model fluxes over each bandpass of the system calibrated to the reference star (Vega) using the following equation (Maíz Apellániz 2007; Al-Wardat 2012)

$$m_p[F_{\lambda,s}(\lambda)] = -2.5 \log \frac{\int P_p(\lambda) F_{\lambda,s}(\lambda) \lambda d\lambda}{\int P_p(\lambda) F_{\lambda,r}(\lambda) \lambda d\lambda} + ZP_p, \quad (9)$$

**Table 6** Orbital Elements, Parallax and Total Mass of the System Gliese 762.1 using Relative Position Measurements

Parameter	Arenou et al. (2000)	Pourbaix (2000)	Farrington et al. (2010)	This work
$P$ (yr)	$1.35458 \pm 0.00131$	$1.352776 \pm 0.00071$	$1.35297 \pm 0.00159$	$1.3534 \pm 0.00075$
$T_0$ (MJD)	$48641.21 \pm 3.10$	$46164.9 \pm 1.66$	$46671.4 \pm 8.5$	$47670.20 \pm 2.37$
$e$	$0.340 \pm 0.013$	$0.3600 \pm 0.0078$	$0.371 \pm 0.006$	$0.36 \pm 0.020$
$a$ (arcsec)	$0.084 \pm 0.003$	$0.0860 \pm 0.0014$	$0.0842 \pm 0.3$	$0.0865 \pm 0.010$
$i$ ( $^\circ$ )	$144.6 \pm 1.7$	$144 \pm 2.4$	$144.0 \pm 1.29$	$140.0 \pm 2.00$
$\omega$ ( $^\circ$ )	$177.8 \pm 2.1$	$356 \pm 2.1$	$16.57 \pm 4.1$	$198.0 \pm 4.4$
$\Omega$ ( $^\circ$ )	$74.6 \pm 6.8$	$243 \pm 1.5$	$256.9 \pm 2.666$	$253 \pm 6.55$
$\pi$ (mas)	$57.99 \pm 0.57$	$57.3 \pm 0.3$	$59.2 \pm 2.04$	$58.96 \pm 0.65^a$
$M$ ( $M_\odot$ )	$1.62 \pm 0.18$	$1.67 \pm 0.83$	$1.59 \pm 0.18$	$1.72 \pm 0.60$

Notes: <sup>a</sup> New Hipparcos (van Leeuwen 2007) (see Table 1).

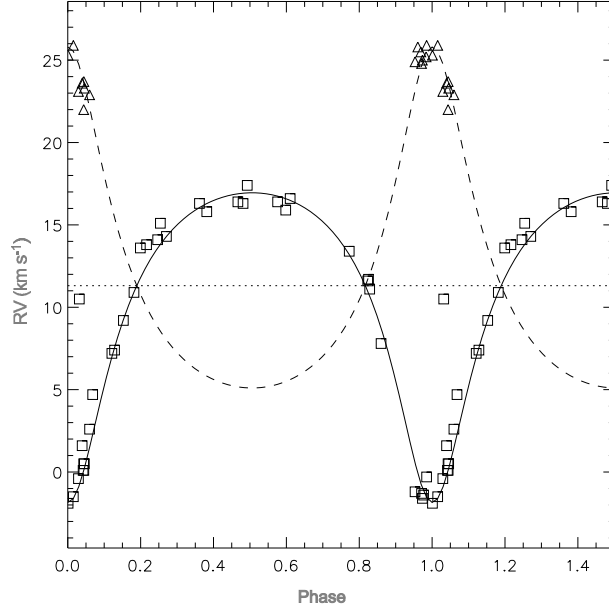


**Fig. 2** Spectroscopic orbital solution for Gliese 762.1 in Table 5 and radial velocities. Triangles represent radial velocities of the primary component and squares represent radial velocities of the secondary component. The dashed line in the figure represents the center of mass velocity ( $V_\gamma = 11.31 \pm 0.12 \text{ km s}^{-1}$ ).

where  $m_p$  is the synthetic magnitude of the passband  $p$ ,  $P_p(\lambda)$  is the dimensionless sensitivity function of the passband  $p$ ,  $F_{\lambda,s}(\lambda)$  is the synthetic SED of the object and  $F_{\lambda,r}(\lambda)$  is the SED of Vega. Zero points ( $ZP_p$ ) from Maíz Apellániz (2007) (and references therein) were adopted.

The results of the calculated magnitudes and color indices (Johnson:  $U, B, V, R, U - B, B - V, V - R$ ; Strömgren:  $u, v, b, y, u - v, v - b, b - y$  and Tycho:  $B_T, V_T, B_T - V_T$ ), of the entire system and individual components, in different photometrical systems, are shown in Table 7.

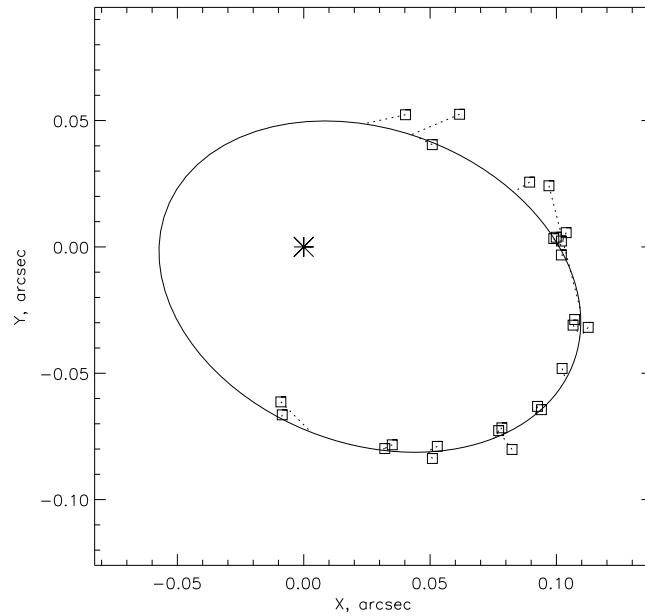
#### 4 RESULTS AND DISCUSSION

Table 8 shows a high consistency between the synthetic magnitudes and colors and the observational ones. This gives a good indication about the reliability of the estimated parameters listed in Table 4. Also, the resulting magnitude difference, individual magnitudes and absolute magnitudes (Tables 4 and 7) are consistent with the calculated ones that are used as preliminary input parameters.

The positions of the components of the system on the evolutionary tracks of Girardi et al. (2000a) (Fig. 4) show that both components, each with masses between 0.8 and 0.9  $M_\odot$ , are main sequence stars, but both show a slight displacement upwards from the zero-age main sequence. Their positions on Girardi et al. (2000a) isochrones for low- and intermediate-mass stars of different metallicities and those of the solar composition [ $Z = 0.019, Y = 0.273$ ] are shown in Figures 5 and 6, which give an age of the system of around  $9 \pm 1$  Gyr.

The spectral types and luminosity classes of both components are assigned as K0V and K1.5V for the primary and secondary components respectively, and their positions on the evolutionary tracks are shown in Figure 4, which are brighter than those given by Farrington et al. (2010) as K2V and K4V.

The estimated orbital elements of the system (Tables 5 and 6) are consistent with previous works. The orbit of the system was solved using a combination of



**Fig. 3** The best visual orbit of the system with the relative position measurements from the Fourth Catalog of Interferometric Measurements of Binary Stars. The asterisk represents the position of the primary component.

**Table 7** Magnitudes and Color Indices of the Synthetic Spectra of the System Gliese 762.1.

Sys.	Filter	Entire $\sigma = \pm 0.02$	Comp. A	Comp. B
Joh-	<i>U</i>	7.99	8.53	9.01
Cou.	<i>B</i>	7.47	8.05	8.43
	<i>V</i>	6.60	7.20	7.53
	<i>R</i>	6.12	6.74	7.03
	<i>U - B</i>	0.52	0.48	0.58
	<i>B - V</i>	0.87	0.85	0.90
	<i>V - R</i>	0.47	0.46	0.50
Ström.	<i>u</i>	9.15	9.69	10.18
	<i>v</i>	7.96	8.52	8.94
	<i>b</i>	7.06	7.65	8.00
	<i>y</i>	6.56	7.16	7.48
	<i>u - v</i>	1.19	1.16	1.24
	<i>v - b</i>	0.90	0.87	0.94
	<i>b - y</i>	0.50	0.49	0.52
	Tycho	<i>B<sub>T</sub></i>	7.71	8.28
	<i>V<sub>T</sub></i>	6.70	7.29	7.63
	<i>B<sub>T</sub> - V<sub>T</sub></i>	1.02	0.99	1.05

the relative position measurements and the radial velocity curves, which gives more reliable and accurate results.

The sum of the masses of the components in the system and the individual masses were calculated and estimated in three different ways; using the physical parameters and standard relations as  $M_A = 0.89 \pm 0.08 M_\odot$ ,  $M_B = 0.83 \pm 0.07 M_\odot$ , using the orbital elements with Hipparcos parallax as  $M_A + M_B = 1.72 \pm 0.60 M_\odot$  and depending on the positions of the components of the system on the evolutionary tracks computed from Girardi et al. (2000a) (Fig. 4) which coincide with the

**Table 8** Comparison between the observational and synthetic magnitudes, colors and magnitude differences of the system Gliese 762.1.

	Observed † (mag)	Synthetic (This work)
<i>V<sub>J</sub></i>	6.60	$6.60 \pm 0.02$
<i>B<sub>J</sub></i>	7.46	$7.47 \pm 0.02$
<i>R<sub>J</sub></i>	6.10	$6.12 \pm 0.02$
<i>B<sub>T</sub></i>	$7.71 \pm 0.01$	$7.71 \pm 0.02$
<i>V<sub>T</sub></i>	$6.71 \pm 0.01$	$6.70 \pm 0.02$
<i>(B - V)<sub>J</sub></i>	$0.86 \pm 0.01$	$0.87 \pm 0.02$
<i>(U - B)<sub>J</sub></i>	$0.52 \pm 0.02$	$0.52 \pm 0.02$
$\Delta m$	$0.33^\ddagger \pm 0.06$	$0.33 \pm 0.04$

Notes: † See Table 1; ‡ Average value for fifteen  $\Delta m$  measurements (see Table 2).

calculated ones. This figure shows positions of the components of the system on the evolutionary tracks of Girardi et al.

Depending on the estimated parameters of the components of the system and their positions on the evolutionary tracks, fragmentation is a possible process for the formation of the system. Bonnell (1994) concludes that fragmentation of a rotating disk around an incipient central protostar is possible, as long as there is continuing infall. Zinnecker & Mathieu (2001) pointed out that hierarchical fragmentation during rotational collapse has been invoked to produce binaries and multiple systems.

It is worthwhile to mention here that the system Gliese 762.1 is a detached case with an orbital period of  $1.3534 \pm 0.0010$  yr. So, this system is visually close but not a contact binary, and if we compare it with other extremely close binary systems having K-type stars like BI

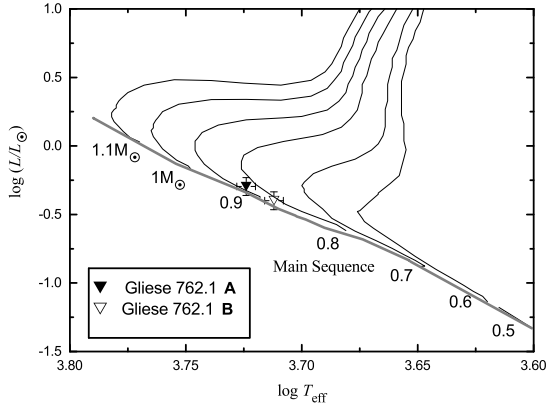


**Fig. 4** The components of the system on the evolutionary tracks with masses (0.5, 0.6, 0.7, ..., 1.1  $M_{\odot}$ ) of Girardi et al. (2000b).

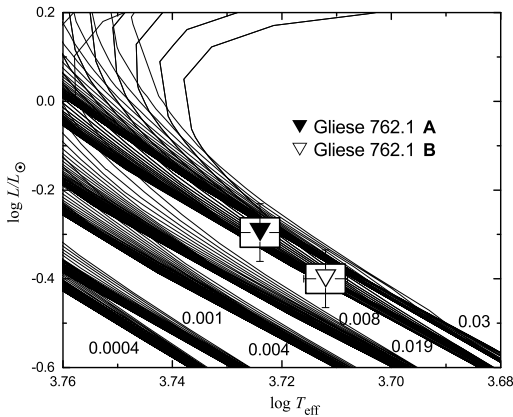


**Fig. 5** The components of the system on the isochrones for low- and intermediate-mass stars with different metallicities as given by Girardi et al. (2000a).

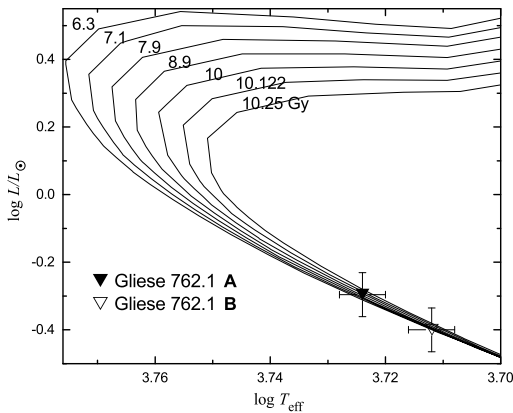


**Fig. 6** The components of the system on the isochrones of low- and intermediate-mass, solar composition [ $Z = 0.019$ ,  $Y = 0.273$ ] stars as given by Girardi et al. (2000a).

Vulpeculae (Qian et al. 2013), AD Cancri (Qian et al. 2007) and PY Virginis (Zhu et al. 2013), which have shorter orbital periods ( $\sim$ days) and lower angular momenta among K-type binary stars, we find that the orbital evolution of such systems is affected by the existence of a third component by removing angular momentum from the central binary system during the early stellar formation process or/and later dynamical interactions. However, as for Gliese 762.1, such dynamical interactions may not exist. It may form directly from the stellar formation process because the orbital separation between the two components is much larger.

## 5 CONCLUSIONS

We present the results of the complex analysis of the double-lined spectroscopic binary system Gliese 762.1. We were able to achieve the best fit between the entire synthetic SED and the observational one (Fig. 1) by producing and calibrating synthetic SEDs of the individual components in an iterative method. The orbit of the system and its radial velocities were also solved to estimate reliable orbital elements consistent with the physical parameters from atmospheric modeling.

We relied on Hipparcos parallax ( $58.96 \pm 0.65$  mas,  $d = 16.96$  pc, van Leeuwen 2007) for the calculations of the entire SED and the masses of components in the system. The Hipparcos parallax was not that far from the dynamical parallaxes introduced in previous orbital solutions (see Table 6).

**Acknowledgements** This research has made use of SAO/NASA, the SIMBAD database, the Fourth Catalog of Interferometric Measurements of Binary Stars, IPAC data systems and the CHORIZOS code of photometric and spectrophotometric data analysis. We would like to thank Jürgen Weiprecht from Astrophysikalisches Institut und Universitäts-Sternwarte, FSU Jena for his help. S. Masda would like to thank the Ministry of Higher Education and Scientific Research in Yemen for the scholarship, and he would like also to thank Hadhramout University (Faculty of Al-Mahra Education).

## References

- Al-Wardat, M. A. 2002a, Bulletin of the Special Astrophysics Observatory, 53, 51
- Al-Wardat, M. A. 2002b, Bulletin of the Special Astrophysics Observatory, 54, 29
- Al-Wardat, M. A. 2007, Astronomische Nachrichten, 328, 63
- Al-Wardat, M. A. 2009, Astronomische Nachrichten, 330, 385
- Al-Wardat, M. 2012, PASA, 29, 523
- Al-Wardat, M. A. 2014, Astrophysical Bulletin, 69, 454
- Al-Wardat, M. A., Balega, Y. Y., Leushin, V. V., et al. 2014a, Astrophysical Bulletin, 69, 58
- Al-Wardat, M. A., Balega, Y. Y., Leushin, V. V., et al. 2014b, Astrophysical Bulletin, 69, 198

- Al-Wardat, M. A., & Widyana, H. 2009, *Astrophysical Bulletin*, 64, 365
- Al-Wardat, M. A., Widyana, H. S., & Al-thyabat, A. 2014c, *PASA*, 31, 5
- Arenou, F., Halbwegs, J.-L., Mayor, M., Palasi, J., & Udry, S. 2000, in *IAU Symposium*, 200, 135
- Arenou, F., Halbwegs, J.-L., Mayor, M., et al. 2002, in *EAS Publications Series*, 2, eds. O. Bienayme, & C. Turon, 155
- Balega, I., Balega, Y. Y., Maksimov, A. F., et al. 2004, *A&A*, 422, 627
- Balega, I. I., Balega, A. F., Maksimov, E. V., et al. 2006, *Bulletin of the Special Astrophysics Observatory*, 59, 20
- Balega, I. I., Balega, Y. Y., Belkin, I. N., et al. 1994, *A&AS*, 105
- Balega, I. I., Balega, Y. Y., Gasanova, L. T., et al. 2013, *Astrophysical Bulletin*, 68, 53
- Balega, I. I., Balega, Y. Y., Hofmann, K.-H., et al. 2002, *A&A*, 385, 87
- Balega, I. I., Balega, Y. Y., Maksimov, A. F., et al. 2007a, *Astrophysical Bulletin*, 62, 339
- Balega, Y. Y., Beuzit, J.-L., Delfosse, X., et al. 2007b, *A&A*, 464, 635
- Batten, A. H., Fletcher, J. M., & MacCarthy, D. G. 1989, *Publications of the Dominion Astrophysical Observatory Victoria*, 17, 1
- Bonnell, I. A. 1994, *MNRAS*, 269
- Duquennoy, A., Mayor, M., & Halbwegs, J.-L. 1991, *A&AS*, 88, 281
- ESA, ed. 1997, *ESA Special Publication*, 1200, *The HIPPARCOS and TYCHO Catalogues. Astrometric and Photometric Star Catalogues Derived from the ESA HIPPARCOS Space Astrometry Mission*
- Farrington, C. D., ten Brummelaar, T. A., Mason, B. D., et al. 2010, *AJ*, 139, 2308
- Forveille, T., Beuzit, J.-L., Delfosse, X., et al. 1999, *A&A*, 351, 619
- Girardi, L., Bressan, A., Bertelli, G., & Chiosi, C. 2000a, *A&AS*, 141, 371
- Girardi, L., Bressan, A., Bertelli, G., & Chiosi, C. 2000b, *VizieR Online Data Catalog*, 414, 10371
- Gray, D. F. 2005, *The Observation and Analysis of Stellar Photospheres*, 515 (UK: Cambridge University Press)
- Hartkopf, W. I., & Mason, B. D. 2009, *AJ*, 138, 813
- Hartkopf, W. I., McAlister, H. A., & Franz, O. G. 1992, *AJ*, 104, 810
- Hartkopf, W. I., McAlister, H. A., Mason, B. D., et al. 1997, *AJ*, 114, 1639
- Hartkopf, W. I., Mason, B. D., McAlister, H. A., et al. 2000, *AJ*, 119, 3084
- Horch, E. P., Gomez, S. C., Sherry, W. H., et al. 2011, *AJ*, 141, 45
- Horch, E. P., Meyer, R. D., & van Altena, W. F. 2004, *AJ*, 127, 1727
- Horch, E. P., Robinson, S. E., Meyer, R. D., et al. 2002, *AJ*, 123, 3442
- Horch, E. P., van Altena, W. F., Cyr, Jr., W. M., et al. 2008, *AJ*, 136, 312
- Ismailov, R. M. 1992, *A&AS*, 96, 375
- Kurucz, R. 1994, *Solar Abundance Model Atmospheres for 0, 1, 2, 4, 8 km s<sup>-1</sup>*, Cambridge, Mass.: Smithsonian Astrophysical Observatory, 19
- Lang, K. R. 1992, *Astrophysical Data I. Planets and Stars*. (Springer-Verlag Berlin Heidelberg New York), 133
- Maíz Apellániz, J. 2007, in *Astronomical Society of the Pacific Conference Series*, 364, *The Future of Photometric, Spectrophotometric and Polarimetric Standardization*, ed. C. Sterken, 227
- McAlister, H. A., Hartkopf, W. I., Gaston, B. J., Hendry, E. M., & Fekel, F. C. 1984, *ApJS*, 54, 251
- McAlister, H. A., Hartkopf, W. I., Hendry, E. M., Campbell, B. G., & Fekel, F. C. 1983, *ApJS*, 51, 309
- McAlister, H. A., Hartkopf, W. I., Hutter, D. J., & Franz, O. G. 1987, *AJ*, 93, 688
- McAlister, H. A., Hartkopf, W. I., Sowell, J. R., Dombrowski, E. G., & Franz, O. G. 1989, *AJ*, 97, 510
- McClure, R. D. 1983, *PASP*, 95, 201
- Pluzhnik, E. A. 2005, *A&A*, 431, 587
- Pourbaix, D. 2000, *A&AS*, 145, 215
- Pourbaix, D., & Jorissen, A. 2000, *A&AS*, 145, 161
- Qian, S.-B., Yuan, J.-Z., Soonthornthum, B., et al. 2007, *ApJ*, 671, 811
- Qian, S.-B., Liu, N.-P., Li, K., et al. 2013, *ApJS*, 209, 13
- Tokovinin, A. 1992, in *Astronomical Society of the Pacific Conference Series*, 32, *IAU Colloq. 135: Complementary Approaches to Double and Multiple Star Research*, eds. H. A. McAlister, & W. I. Hartkopf, 573
- Tokovinin, A. A. 1985, *A&AS*, 61, 483
- Tokovinin, A. A., & Ismailov, R. M. 1988, *A&AS*, 72, 563
- van Leeuwen, F. 2007, *A&A*, 474, 653
- Zhu, L. Y., Qian, S. B., Liu, N. P., Liu, L., & Jiang, L. Q. 2013, *AJ*, 145, 39
- Zinnecker, H., & Mathieu, R., eds. 2001, *IAU Symposium*, 200, *The Formation of Binary Stars*